ANALYSIS OF TRITIUM/DEUTERIUM RETENTION AND PERMEATION IN FW/DIVERTOR INCLUDING GEOMETRIC AND TEMPERATURE OPERATING FEATURES

Alice Ying, Haibo Liu, Mohamed Abdou

Mechanical and Aerospace Engineering Department, UCLA, Los Angeles, CA 90095, USA
ying@fusion.ucla.edu

Available data and mathematical formulations concerning tritium transport in the FW/Divertor with tungsten and beryllium as plasma facing materials were implemented in the commercial code COMSOL Multiphysics. The goal is to develop a CAD-based multiphysics modeling capability so that FW/Divertor temperature and geometric features can be readily taken into consideration while tritium permeation to the primary coolant in a prototypical PFC can be more realistically addressed. This development began with the simulation of ion implantation experiments, validated against existing laboratory experimental results. Analysis shows that with ITER FW where Be is used as the plasma facing material, the low operating temperature, erosion, and the dwell time greatly hinder tritium bulk diffusion, permeation, and inventory accumulation. However, under DEMO high-temperature operating conditions, tritium can quickly diffuse through tungsten to structural material and reach a steady state inventory after a relatively short time. Additionally, its permeation to the coolant can be reduced when the Soret effect is considered. The findings and challenges of developing a 3-D predictive capability for tritium transport in a FW/Divertor PFC are discussed.

I. INTRODUCTION

Tritium in the in-vessel component primary coolant stream can either come from tritium implanted in the plasma facing component (PFC) or tritium generated inside the breeder zones of the blanket. The ability to estimate the tritium permeation rate from the PFC to the first wall (FW) coolant by tritium diffusion through the coolant containing structures is important to the construction of tritium self-sufficiency criteria. Tritium permeation characteristics and quantity in a PFC are governed by many factors, including the tritium implantation profile, temperature dependent diffusion terms, defect production and consequent tritium trapping and de-trapping, and multiple hydrogen /tritium species and chemical compositions. As the data have shown, tritium has a higher solubility in ITER or DEMO heat sink materials such as CuCrZr and F82H than in tungsten or beryllium under prototypical operating temperature regimes. Even the temperature profile enhances the tritium ability to diffuse toward the frontal surface due to thermo diffusion effect; because of this high solubility, tritium could still move to the heat sink substrate and permeate into the coolant. A better account of tritium inventory in the plasma facing components such as the first wall (FW) and divertor should incorporate the heat sink substrates. Furthermore, laboratory deuterium/ tritium thermal desorption experiments have shown that the retained deuterium/tritium in tungsten desorbed at temperatures of ~450 K, ~650 K and ~790 K for neutron induced trap.[1-2] These temperatures are in the ranges of DEMO operations, which indicate that the trapped tritium can simultaneously de-trap during operations.

There are several one-dimensional codes that simulate these properties in typical plasma facing materials, like TMAP4 and TMAP7 (Ref. 3) from the US and TPERM (Ref. 4) from Japan. Moreover, a fair amount of experimental work has been conducted to study ion implanted deuterium/tritium inventories and the effects of ion induced defects and intrinsic defects on tritium retention and desorption using simple samples. While 1-D models have been performed and fit reasonably well with experimental data, mostly integral retained quantities have been predicted and compared with the thermodesorption spectroscopy (TDS) results. The evolution concerning deuterium/tritium mitigation among the bulk, intrinsic or ion induced trap concentration was not well simulated. In this paper, available data and mathematical formulation[1,3] from the literatures concerning tritium transport in FW/Divertor with tungsten and beryllium as plasma facing materials are reconstructed in the commercial code COMSOL Multiphysics[5] so that the temperatures and tritium transport in a prototypical FW/Divertor can be realistically incorporated and considered. The ultimate goal of this work is to build a multi-dimensional, multiphysics tritium predictive modeling capability, which can more accurately simulate retention and permeation quantities in a complex PFC engineering

component. The first step of the work taking into account the geometry and temperature distribution of a FW PFC in 1- and 2-D, including the effects of ion-induced and intrinsic defects is presented here in this paper. The model is being built starting from simple 1-D geometry, proceeding to increasingly complex geometries and operating conditions, and calculations are benchmarked with existing data.

II. TRITIUM TRANSPORT MECHANISMS AND IMPLEMENTATION IN COMSOL

The tritium transport in solid metal is determined by several mechanisms. 1) The diffusion coefficient and the solubility describe how fast the tritium atoms hop through the metal and how many of them are hopping, respectively. In the diffusion process, the tritium will be retained in the metal as solute atoms. 2) Tritium trapping sites will trap tritium and increase retention in the metal. There are three kinds of trap mechanisms: trapping due to material intrinsic defects, trapping due to ion induced defects and trapping due to neutron damage. The trap site produced by ion implantation is limited to a nanometer beneath the surface, and is generally modeled using a Gaussian distribution profile. The intrinsic defects and neutron damage induced trap sites are throughout the material bulk. 3) The tritium retention will also be impacted by plasma facing surface effects, which include surface erosion, deposition, and consequent surface topography alteration. 4) The Soret effect will decrease tritium retention and permeation if the diffusion species has a negative heat of transport, which is the case for steel.

The above physics-based models are implemented into the multiphysics code COMSOL to simulate tritium transport in a fusion reactor FW/Divertor PFC. The tritium transport process is governed by equation (1) (Refs. 1,3), where $C(x,t)$ is the solute tritium concentration, $J(x,t)$ is the diffusive flux, I_0 is the implanted tritium ion flux density from plasma, $\Phi(x)$ is the tritium implantation profile and $Y(x,t)$ is the trapped tritium concentration. The diffusive flux $J(x,t)$ is described by equation (2) (Refs. 3,6), where D is the diffusion coefficient and Q is the heat of transport. The diffusion coefficient is defined in equation (3), where D_0 is the pre-exponential factor, E_a is the diffusion activation energy and k is Boltzmann constant. The tritium implantation profile is described by a Gaussian distribution function, as defined in equation (4) (Ref. 6), where A is defined in equation (5). R_p and $\langle \Delta x^2 \rangle$ are the mean implantation depth and its variance, respectively. The trapped tritium concentration dynamic equation in metal is described by equation (6) (Ref. 3), where a is the metal lattice constant, $W(x,t)$ is the density of traps and E_b is the binding energy of tritium with a trap, which is defined as the difference between the trap energy E_t and the activation energy E_a. The energy conservation is described by equation (7), where ρ is the material density, C_p is the heat capacity, k is the thermal conductivity, h is the convective heat transfer coefficient, T_{ext} is the external temperature and q is the heat source.

$$\frac{\partial C(x,t)}{\partial t} + \nabla \cdot J(x,t) = (1-r) I_0 \varphi(x) - \frac{\partial Y(x,t)}{\partial t} \quad (1)$$

$$J(x,t) = -D(\nabla C(x,t) + \frac{QC(x,t)}{RT^2}\nabla T) \quad (2)$$

$$D = D_0 \exp(-E_a / kT) \quad (3)$$

$$\varphi(x) = A \exp(-(x-R_p)^2 / (2\langle \Delta x^2 \rangle)) \quad (4)$$

$$A = 1 / \int_0^L \exp(-(x-R_p)^2 / (2\langle \Delta x^2 \rangle) dx \quad (5)$$

$$\frac{\partial Y(x,t)}{\partial t} = (2Da/3)(C(x,t)(W(x,t) - Y(x,t)) - (12Y(x,t)/a^3)\exp(-E_b/kT)) \quad (6)$$

$$\rho C_p \frac{\partial T}{\partial t} - \nabla \cdot (k \nabla T) = q + h(T_{ext} - T) \quad (7)$$

The boundary conditions (BCs) on the plasma facing side and coolant side are recombination BCs, given by equation (8). K_r is the recombination coefficient, which is defined in equation (9), where K_{r0} is the pre-exponential factor and E_r is the recombination energy.

$$J(x) = -2K_r C(x)^2 \quad (8)$$

$$K_r = K_{r0} \exp(-E_r / kT) \quad (9)$$

On modeling the PFC-steel interface, the stiff-spring method is used. This BC defines continuous flux conditions cross the interface while allowing for the concentrations to satisfy Sieverts' law.

For modeling tritium transport in COMSOL, reliable data for the diffusion coefficient, the recombination rate coefficient, the trap densities and activation energies are needed, which are selected from literature. Most of the data were derived for deuterium, and there is not yet an effort to differentiate the difference caused by isotope effect.

III. MODEL VALIDATIONS

III.A. Deuterium/Tritium Retention in Tungsten

In the 1-D implementation, simulations were performed of selective laboratory ion implementation experiments using tungsten and Be as targeted plasma facing materials. Large differences exist among the available recombination rate coefficient data, such as data from Andrel et al. (Ref. 7) and from Pick and Sonnenberg.[8] Understanding the significance of the

differences may guide further research. A tungsten layer with 6 mm thickness is simulated with deuterium implantation at 300 K. A fourteenth order of magnitude difference in recombination rate coefficients between these two predictions resulted in about a 8.8% difference in the amounts of the total retained deuterium/tritium (8.21×10^{20} versus 7.45×10^{20} D/m^2) at lower incident flux of 3×10^{21} m^{-2}s^{-1}. For this ion flux, a more pronounced difference is in the concentration profile. As illustrated in Fig. 1, the ion induced trap concentration profile right beneath the surface is much higher for a lower recombination rate coefficient, as predicted by Andrel et al. (Ref. 7).

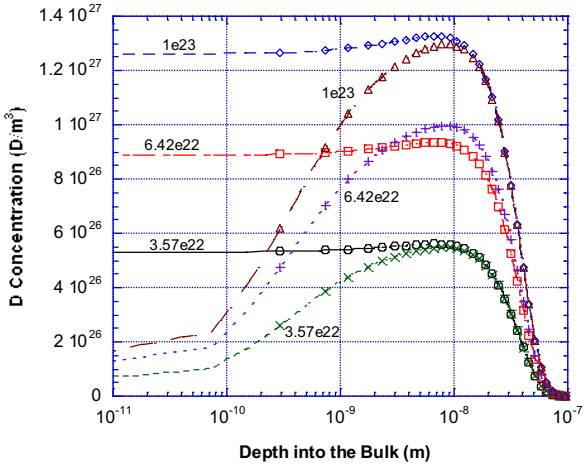

Fig. 1. Deuterium concentration profiles in ion-induced traps in tungsten for different recombination rate coefficients and different fluencies (◊, □, ○: Andrel; Δ, +, x: Pick).

The difference in the calculated retained deuterium decreases to less than 2% at higher incident ion flux of > 1×10^{22} m^{-2}s^{-1}. Fig. 2 summarizes the calculated retained deuterium quantities as a function of ion fluence under an incident flux of 1.2×10^{22} m^{-2}s^{-1} at two different implantation temperatures 500 K and 623 K. The analysis was for ion energy of 200 eV, an implantation range of 5.9 nm, and an assumed standard deviation of 5.8 nm. The calculated results fall between the upper and lower bounds of the predicted values of the experimentally derived correlations (Y_1 and Y_2 are fitted upper and lower implanted deuterium retention limit curves as a function of implanted fluence x taken from Ref. 9), and are closer to the upper predicted values.

III.B. Deuterium TDS Experiment in Tungsten

Thermodesorption flux calculations using trapping parameters presented in (Ref. 1) capture temperature dependent D released characteristics. In this experiment, 200 eV D^+ is implanted to tungsten in room temperature. The implant flux is 3.2×10^{19} D m^{-2}s^{-1} and the fluence is 1×10^{23} D/m^2. The intrinsic traps atom fraction is 4×10^{-4} and the ion-induced traps atom fraction is 0.1. The instrinsic trap energy is 0.85 eV (Ref. 1). However, the released peak at 600 K was reproduced with trap energy of 1.50 eV rather than that of 1.45 eV as used in the paper (Fig. 3).

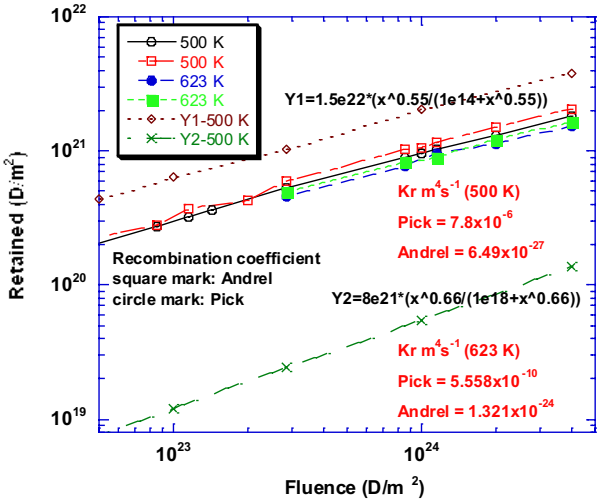

Fig. 2. Retained deuterium in tungsten as a function of fluence at two different implantation temperatures and compared with the available correlations.

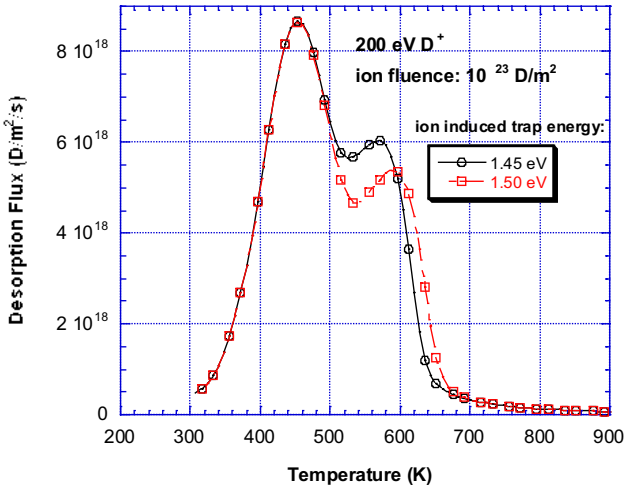

Fig. 3.Thermodesorption spectra after an ion plasma implantation experiment (Tungsten).

III.C. Erosion and Codeposition Effects in Beryllium

As has been pointed out in the literature, erosion and codeposition are the major issues for Be, dominating tritium retention characteristics. The erosion removes deposited deuterium/tritium from the plasma facing surface and significantly reduces the amount of retained deuterium/tritium. The experimental results have also shown that the retained tritium/deuterium reached its

saturated value, formed porous structures, and enhanced the return of the implanted ions to the plasma. Deuterium/tritium removal from a Be PFC due to erosion must be included in the model to account for the lower retention found in experiments. In literature, this is modeled by equation (10) (Ref. 10):

$$J_r = -(2K_r n_o^2 + u n_o) \quad (10)$$

Where u is erosion face velocity. A model same as the one in Ref. 10 is simulated. The beryllium samples implanted with deuterium ion under 200 ^oC and 500 ^oC are thermal desorbed to 650 ^oC. The ion energy is 100 eV and the flux is $1.8x10^{21}$ $m^{-2}s^{-1}$ for 200 ^oC and $1.5x10^{22}$ $m^{-2}s^{-1}$ for 500 ^oC. As illustrated in Fig.4, without taking into account the erosion effect the calculation predicts a much higher retained quantity than that shown in the experimental data. The experimental results can be nearly reproduced when a term representing the erosion effect is included as the boundary flux in addition to the enhanced recombination flux due to saturation. The moving surface effect is not included in this model and it will be explored in the following study.

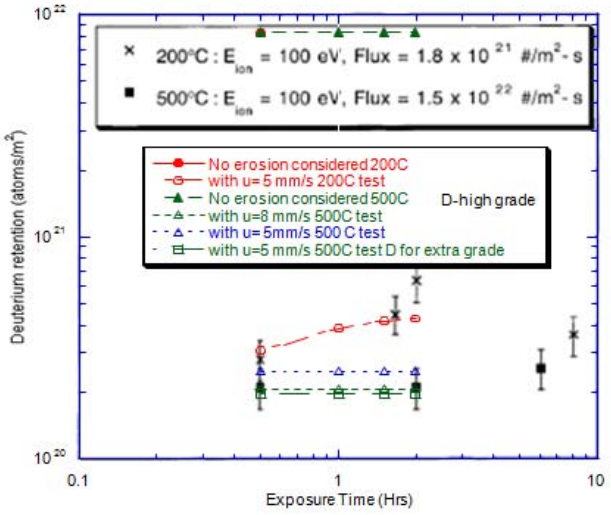

Fig. 4. Calculated deuterium retention overlaid on top of the experimental data of Doerner, et al. (Ref. 11)

IV. 2-D MODELING WITH OPERATIONAL CHARACTERISTICS

IV.A. ITER NHF FW

The aforementioned validations show that COMSOL can properly model the underlying physics involved in tritium transport in a FW/Divertor component. Before moving beyond 1-D simulations, the capability of COMSOL to model a prototypical FW/Divertor geometry and operating conditions must be addressed. As the first test case, tritium transport in a 2-D unit cell of the ITER normal heat flux (NHF) FW design is studied. The NHF FW incorporates a 1 cm thick Be plasma facing material, and a 1 mm thick SS liner brazed into the hole embedded in the 24 mm thick CuCrZr heat sink for the cooling water flowing through to remove the heat. Under ITER operating conditions, Be surface temperature remains relatively low (< 220 ^oC) except for a small region that is subjected to a high convective flux. The low temperature and the saturation effect limit the amount of deuterium/tritium diffusing to the bulk and provide a favorable effect on tritium inventories and permeation rates to coolant streams. For a 1-cm thick Be tile, it may take more than 30,000 cycles of ITER inductive operations for tritium to diffuse to the Be/CuCrZr interface under ITER operating temperatures using high diffusivity estimated for the extra-grade Be. This is illustrated in Fig. 5, where the tritium flux has not yet reached 1 mm after 2501 cycles of operations.

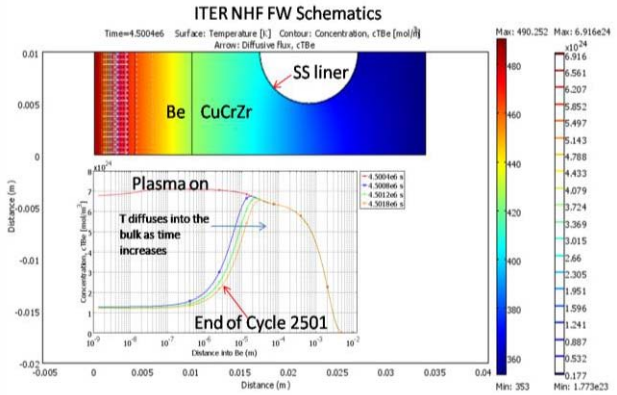

Fig. 5. Calculated temperature and tritium concentration profiles in Be for the ITER NHF FW.

IV.B. DEMO FW

The effect of higher temperature operations is examined for a prototypical DEMO FW configuration. The 2-D FW schematics incorporate a 2-mm tungsten plasma facing layer followed by a RAFS (reduced activation ferritic steel) rectangular cooling channel.[12] The tungsten operates at temperature gradients between 550 and 650 ^oC while the RAFS structure between 300 and 550 ^oC with a DEMO neutron wall load of 3.7 MW/m^2 and a surface heat flux of 0.7 MW/m^2. As shown by Longhurst[12] and G. V. Ogorodnikova et al. (Ref. 6), under a temperature gradient, diffusion could occur up-hill against the concentration gradient as long as it leads to a reduction of the Gibbs energy in the system. This effect is also known as thermal diffusion or the Ludwig-Soret effect. The Soret effect can dominate the concentration profiles and has a profound effect on tritium permeation rates and retention for fusion reactor structures. The influence of Soret effect on tritium

permeation is examined here. The formula used to calculate iron heat of transport is -74050+58.3*T J/mol taken from (Ref. 13). Temperature dependent physical properties are used for tungsten and RAFS.[14] Recombination boundary conditions were applied to the coolant channel boundaries. The diffusive flux vector plot shown in Fig. 6 reflects how boundary conditions control diffusive fluxes. The Soret effect resisted tritium to diffuse to RAFS and resulted in a lower tritium concentration magnitude in RAFS. The impact of the Soret effect on tritium diffusive flux and concentration profile in RAFS is further shown in Fig. 7.The amount of retained tritium in RAFS ends up about 34% higher while the permeation is ~ 50% higher when Soret effect is not taken into consideration.

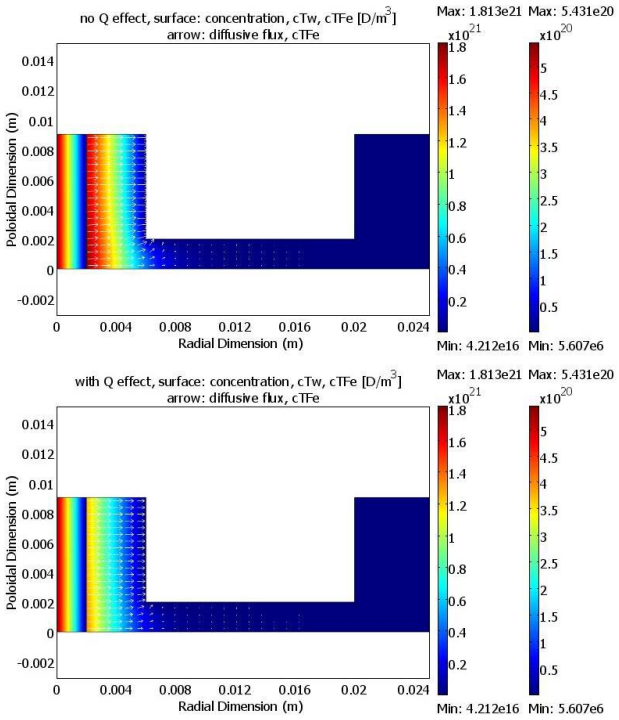

Fig. 6. Calculated 2D DEMO tritium concentrations in both tungsten and RAFS structure and diffusive flux in RAFS with (bottom) and without (top) Soret effect (The left legend is for tungsten, while the right is for RAFS).

The effect of higher tritium solubility in the RAFS[15] (as compared to tungsten or Be) is reflected in a jump in the tritium concentration amplitude at the W/RAFS interface, as shown in Fig. 7. The jump is decreased by Soret effect indicating a less tritium diffusion toward RAFS side. For the case studied, tritium inventory reaches its saturated value at about 1500 s in tungsten, but it takes about 3000 s for RAFS.

IV.C. Ion-Induced Traps Effect

The ion-induced trap evolution was not considered in the aforementioned 2-D analysis due to a large computing time needed. 1-D analysis incorporating both ion-induced and intrinsic traps was performed to evaluate the differences in the 2-D calculation where this effect was neglected. Calculated 1D with ion-induced trap and 2D tritium inventory (the y direction is normalized to 1 m in order to compare the results with 1D results) evolutions are plotted in Fig. 8. As it is shown, 2-D under estimated the total retained tritium inventory in tungsten by about 30%, which is mainly due to the ion-induced trap. The difference in mobile tritium inventory between 1-D and 2-D calculations is only about 8.8%. This implies that 2-D calculation underestimated tritium activities in RAFS of about 8.8%.

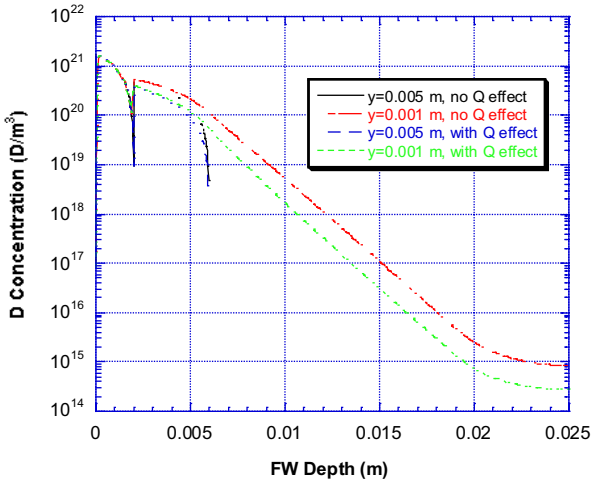

Fig. 7. Deuterium concentration profile along the FW at two different toroidal paths (y).

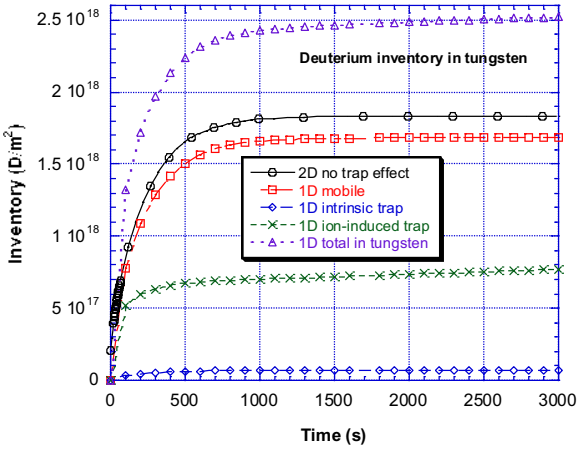

Fig. 8. 1D with traps & 2D no traps (y direction is normalized to 1 m) deuterium inventory in tungsten, no Soret effect in both calculations.

V. OBSERVATION AND SUMMARY

Progress has been made in creating a tritium transport modeling tool using the commercial multiphysics code COMSOL. The intention was to explore and define a CAD-based multiphysics modeling capability for tritium migration and transport studies in a prototypical FW/Divertor geometry without spending an extensive effort on numerical algorithms development. The COMSOL model incorporates the major underlying physics for tritium transport that have been revealed in tungsten and Be plasma facing material experiments. The model was benchmarked against several laboratory experimental results.

The effort so far reveals that it can be time consuming to perform a true 3-D calculation because of the large differences in the length scales over which events take place. Specifically, most implantation driven events occur in an extremely short distance in the range of nanometer for ion implantation and ion-induced damage as compared to the dimensions in other domains such as the overall geometry, temperature gradient, etc. The 3-D calculation is important for DEMO conditions where bulk damage such as caused by radiation[16] dominates tritium retention and the temperatures are higher, allowing tritium to readily diffuse, de-trap and permeate to the coolant streams. To remedy this, a heretical modeling technique incorporating both 1-D, to resolve ion-implanted concentration, induced trapping, de-trapping profiles and associated magnitudes, and 3-D, to solve tritium diffusion and permeation with respect to temperature gradients and geometric boundaries, may be necessary. Additionally, surface topography of the PFC may change as plasma operations continue. However, from a practical engineering point of view, the surface condition of the PFC should be cleaned and maintained regularly (such as annually). The details needed to model the geometry deformation, caused by erosion/co-deposition, in order to predict an accurate global tritium property is yet to be assessed.

ACKNOWLEDGMENTS

This work was jointly supported by the U. S. Department of Energy Contract DE-FG03-ER52123.

REFERENCES

1. O. V. OGORODNIKOVA, et. al., "Deuterium Retention in Tungsten in Dependence of the Surface Conditions," *J. Nucl. Mater.,* **313-316**, 469-477 (2003).
2. YASUHISA OYA, et al., "Comparison of Deuterium Retention for Ion-Irradiated and Neutron-Irradiated Tungsten," Physica Scripta, T145 (2011).
3. G. R. LONGHURST, D. F. HOLLAND, J. L. JONES, AND B. J. MERRILL, June 12, 1992, *TMAP4 User's Manual*, EGG-FSP-10315.
4. K. NAKAHARA, Y. SEKI, JAERI-M 87-118, 1987.
5. COMSOL, 2008. COMSOL, Inc., COMSOL Multiphysics User's Guide, Version 3.5a, Burlington, MA.
6. O.V. OGORODNIKOVA, M.A. FÜTTERER, E. SERRA, G. BENAMATI, J.-F. SALAVY, G. AIELLO, "Hydrogen Isotope Permeation Through and Inventory in the First Wall of the Water Cooled Pb-17Li Blanket for DEMO," *J. Nucl. Mater.,* **273,** 66-78 (1999).
7. R. A. ANDREL et al., *Fusion Technol.,* **21**, 745 (1992).
8. M.A. PICK, K. SONNENBERG, *J. Nucl. Mater.,* **131**, 208 (1985).
9. B. LIPSCHULTZ et al., "An Assessment of the Current Data Affecting Tritium Retention and its Use to Project Towards T Retention in ITER," PSFC/RR-10-4, Plasma Science and Fusion Center, MIT, Cambridge, MA,USA, April 2010
10. G. R. LONGHURST, R. A. ANDREL, R. A. CAUSEY, G. FEDERICI, A. A. HAASZ, R. J. PAWELKO, "Tritium Saturation in Plasma-Facing Materials Surfaces," *J. Nucl. Mater.,* **258-263**, 640-644 (1998).
11. R. P. DOERNER et al., Response of Beryllium to Deuterium Plasma Bombardment, *J. Nucl. Mater.,* **257**, 51-58 (1998).
12. Y. CHEN, et al., The EU Power Plant Conceptual Study – Neutronic Design Analyses for Near Term and Advanced Reactor Models, FZKA 6763, 2003.
13. G. R. LONGHURST, "The Soret Effect and Its Implications for Fusion Reactors," *J. Nucl. Mater.,* **131**, 61-69 (1985).
14. E. SERRA, A. PERUJO, "Influence of the Surface Conditions on Permeation in the Deuterium-MANET System," *J. Nucl. Mater.,* **240**, 215-220 (1997)
15. S., G. BENAMATI, O. V. OGORODNIKOVA, "Hydrogen Isotopes Transport Parameters in Fusion Reactor Materials," *J. Nucl. Mater.,* **255**, 105-115 (1998).
16. M. SHIMADA, et al., "First Result of Deuterium Retention in Neutron-Irradiated Tungsten Exposed to High Flux Plasma in TPE," *J. Nucl. Mater.,* **415**, 667-671 (2011).